Bioenergetic defect associated with mKATP channel opening in a mouse model carrying a mitofusin 2 mutation

Guillet, Virginie; Gueguen, Naïg; Cartoni, Romain; Chevrollier, Arnaud; Desquiret, Valérie; Angebault, Claire; Amati-Bonneau, Patrizia; Procaccio, Vincent; Bonneau, Dominique; Martinou, Jean-Claude; Reynier, Pascal

How to cite

GUILLET, Virginie et al. Bioenergetic defect associated with mKATP channel opening in a mouse model carrying a mitofusin 2 mutation. In: The FASEB journal, 2011, vol. 25, n° 5, p. 1618–1627. doi: 10.1096/fj.10-173609

This publication URL: https://archive-ouverte.unige.ch/unige:17564

Publication DOI: 10.1096/fj.10-173609

Bioenergetic defect associated with mK_{ATP} channel opening in a mouse model carrying a mitofusin 2 mutation

Virginie Guillet,[*,†,‡,1] Naïg Gueguen,[*,‡,1,2] Romain Cartoni,[§,‖,¶] Arnaud Chevrollier,[*,‡] Valérie Desquiret,[‡] Claire Angebault,[*,†] Patrizia Amati-Bonneau,[*,‡] Vincent Procaccio,[*,†,‡] Dominique Bonneau,[*,†,‡] Jean-Claude Martinou,[§] and Pascal Reynier[*,†,‡]

[*]Unité Mixte de Recherche (UMR) Centre National de la Recherche Scientifique (CNRS) 6214, Institut National de la Santé et de la Recherche Médicale (INSERM) U771, Angers, France; [†]School of Medicine, University of Angers, Angers, France; [‡]Department of Biochemistry and Genetics, University Hospital of Angers, Angers, France; [§]Department of Cell Biology, University of Geneva, Geneva, Switzerland; and [‖]F. M. Kirby Neurobiology Center, Children's Hospital, and [¶]Department of Neurology, Harvard Medical School, Boston, Massachusetts, USA

ABSTRACT **Charcot-Marie-Tooth disease type 2A (CMT2A) is an autosomal dominant axonal form of peripheral neuropathy caused by mutations in the mitofusin 2 gene (*MFN2*), which encodes a mitochondrial outer membrane protein that promotes mitochondrial fusion. Emerging evidence also points to a role of MFN2 in the regulation of mitochondrial metabolism. To examine whether mitochondrial dysfunction is a feature of CMT2A, we used a transgenic mouse model expressing in neurons a mutated R94Q form of human MFN2 shown to induce a CMT2A phenotype. Oxygraphic and enzymatic measurements both revealed a combined defect of mitochondrial complexes II and V (40 and 30% decrease, respectively) in the brain of Tg-R94 mice, leading to a drastic decrease of ATP synthesis. These deficiencies were reversed by the mitochondrial ATP-sensitive potassium channel (mK_{ATP}) inhibitor 5-hydroxydecanoate. Conversely, in controls and wild-type human MFN2 mice, the mK_{ATP} activator diazoxide mimicked the deficiency observed with the R94Q mutation. The physical links between complexes II and V, previously proposed as part of mK_{ATP}, were reinforced in Tg-R94Q mice. Our results show that the R94Q MFN2 mutation induces a combined defect of complexes II and V linked to the opening of mK_{ATP}, which could participate in the pathophysiology of the disease.—Guillet, V., Gueguen, N., Cartoni, R., Chevrollier, A., Desquiret, V., Angebault, C., Amati-Bonneau, P., Procaccio, V., Bonneau, D., Martinou, J.-C., Reynier, P. Bioenergetic defect associated with mK_{ATP} channel opening in a mouse model carrying a mitofusin 2 mutation. *FASEB J.* 25, 1618–1627 (2011). www.fasebj.org**

Key Words: Charcot-Marie-Tooth type 2A · succinate dehydrogenase · F0F1-ATP synthase · mitochondria · potassium channel

Charcot-Marie-Tooth disease (CMT) consists of a group of inherited peripheral motor and sensory neuropathies (1), generally characterized by progressive muscular atrophy and weakness with sensory loss in the distal extremities of the limbs. CMT2A (MIM 609260), the most common axonal form of the disease, is mainly caused by mutations in the *MFN2* gene (2). This gene encodes the dynamin GTPase mitofusin 2 (MFN2) located in the outer mitochondrial membrane (3, 4).

Mitochondria are highly dynamic organelles that undergo continuous cycles of fission and fusion. Together with MFN1 and the optic atrophy 1 protein (OPA1), MFN2 plays a major role in the mitochondrial fusion process in mammalian cells (3–5).

Due to the polarity of neurons, with long axons and dendrites, high energy levels are often required far from the soma. Mitochondrial transport and distribution patterns are thus particularly crucial for neurons. Abnormal accumulations of mitochondria have been observed in the distal axon of sural nerve biopsies of patients with CMT2A (6, 7), and mitochondrial aggregations around the nucleus have also been found in mouse embryonic fibroblasts and dorsal root ganglion neurons expressing some CMT2A disease mutations (8, 9). Mitochondrial morphology was not affected in fibroblasts of CMT2A patients carrying a *MFN2* mutation (10, 11); however, these mitochondria demonstrated a decrease in efficiency of oxidative phosphorylation (OXPHOS) and in membrane potential ($\Delta\Psi_m$; ref. 10). Moreover, down-regulation of *MFN2* in L6E9 myotubes has been shown to induce a reduction in

[1] These authors contributed equally to this work.

[2] Correspondence: Laboratoire de Biochimie et Biologie moléculaire, CHU Angers, F-49000, France. E-mail: naiggueguen@yahoo.fr

doi: 10.1096/fj.10-173609

This article includes supplemental data. Please visit *http://www.fasebj.org* to obtain this information.

0892-6638/11/0025-1618 © FASEB

glucose oxidation and $\Delta\Psi_m$ (12, 13). These mitochondrial defects provide additional evidence of the role of MFN2 in cell bioenergetics (14).

Recently, a transgenic mouse model of CMT2A has been generated by expressing in neurons a human cDNA carrying the MFN2 p.R94Q mutation (Tg-R94Q; ref. 15). This particular missense mutation, located immediately upstream of the GTPase domain of MFN2, has been reported in 7 unrelated patients affected by CMT2A (2, 6, 16, 17). Tg-R94Q mice show the main clinical symptoms encountered in patients with CMT2A, namely locomotor impairment and grip-strength defect, whereas no abnormalities were observed in transgenic mice expressing the wild-type human MFN2 (Tg-WT). Tg-R94Q mice also presented an axonal atrophy in the distal sciatic nerve preferentially affecting myelinated axons >3.5 μm in diameter, thereby increasing the proportion of smaller axons. Interestingly, the number of mitochondria per axon was significantly higher in the distal part of these axons than in the larger axons.

In Tg-R94Q mouse embryonic fibroblasts, mitochondrial fusion is maintained by the interaction of MFN2 p.R94Q with MFN1 (8). To address the question of a bioenergetic impairment in the pathogenesis of CMT2A, we compared oxidative phosphorylation and respiratory chain activity in isolated mitochondria from the brain tissue of Tg-R94Q mice with that in Tg-WT and control mice.

MATERIALS AND METHODS

Animals

The human MFN2 mutation p.R94Q was expressed in the nervous tissue of C57BL6 mice to constitute a CMT2A transgenic mouse model having a motor defect. The R94 residue is located immediately upstream of the GTPase domain of MFN2. Human and mouse MFN2 are 95% identical, and all the residues that were found mutated in the original CMT2A study, including p.R94Q (2), are conserved in mouse MFN2 (8). C57BL6 mice, with the human *MFN2* transgene (Tg-Wt: mitoCharc0; ref. 15) or with the mutated human *MFN2* p.R94Q transgene (Tg-R94Q: mitoCharc1; ref. 15) were used; all were obtained from the Department of Cell Biology, University of Geneva. C57BL6 and Tg-Wt mice were used as controls to specifically study the effect of the p.R94Q mutation. Transgenic mice were generated by oocyte injection of human *MFN2* cDNA carrying the p.R94Q mutation. Transgene expression was targeted to differentiated neurons by the neuron-specific enolase promoter. Transgenic animals were identified by PCR analysis, and transgene expression was confirmed by real-time quantitative RT-PCR in the principal cerebral tissues (15). The expression levels of human *MFN2* transgenes in the cortex represented 1/5 of mouse *MFN2* endogenous expression, *i.e.*, in both Tg-Wt and Tg-R94Q mice the *MFN2* expression level (endogenous and exogenous) was 1.2 times that of *MFN2* in control mice (not shown).

Mitochondrial isolation from mouse brain tissue

Mice (age 7 to 9 mo) were anesthetized with isoflurane, in accordance with European Community Guidelines (directive 86/609/CEE), before decapitation and dissection of the cerebral cortex. The isoflurane volume inhaled was strongly controlled and identical for each animal; moreover, preliminary experiments made without the anesthetic showed that the isoflurane volume used had no effect on the mitochondrial parameters investigated, even in Tg-R94Q mice.

The cerebral cortex was diced in 1 ml isolation buffer I/100 mg brain (250 mM sucrose, 10 mM Tris-HCl, 1 mM EDTA, and 0.25 mg/ml fatty acid-free BSA, pH 7.4) before homogenization with 11 up-and-down strokes in a 50-ml potter and 3 up-and-down strokes in a 10-ml tight-fit potter at 1000 rpm. Cell debris were pelleted at 3200 *g* for 10 min, and the supernatant was collected, filtered through gauze, and centrifuged at 10,000 *g* for 10 min. The mitochondrial pellet was washed with buffer I and centrifuged at 6500 *g* for 10 min before resuspension in 0.3 ml of buffer R (250 mM sucrose, 2 mM EDTA, and 20 mM Tris-base, pH 7.4) and conserved on ice. The entire operation was performed at 4°C and completed in <1 h.

Mitochondrial respiratory rates

Brain mitochondria were resuspended in respiratory buffer (225 mM sucrose, 10 mM Tris-HCl, 5 mM KH_2PO_4, 10 mM KCl, 1 mM EDTA, 4 mM $MgCl_2$, and 0.1 mg/ml fatty acid-free BSA, pH7.4). Mitochondrial oxygen consumption was measured at 37°C using a 2-channel, high-resolution Oxygraph respirometer (Oroboros, Innsbruck, Austria). Resting respiration (state 2) was initiated in the presence of either complex I substrate (5 mM malate and 2.5 mM pyruvate) or complex II substrate (5 mM succinate supplemented with 10 μM rotenone), and then maximal ADP-stimulated respiration (state 3) was measured with one addition of saturating ADP concentration (0.5 mM). Cytochrome *c* was added (8 μM) to check outer mitochondrial membrane integrity. Finally, in one oxygraphic chamber, 2 μg/ml oligomycin was added (state 4), and the capacity of the electron transport system was recorded by uncoupling respiratory chain using 1 μM carbonyl cyanide 4-(trifluoromethoxy)phenylhydrazone (FCCP). The respiratory control ratio (RCR), defined as state 3/state 4, was used to evaluate the coupling of respiration to phosphorylation. In the second chamber, antimycin was added, and COX-linked respiration was analyzed using 50 mM ascorbate and 5 mM *N,N,N′,N′*-tetramethyl-*p*-phenylenediamine as substrates. The effects of diazoxide (DZX) and 5-hydroxydecanoate (5HD) on succinate-driven respiration was analyzed on brain mitochondria (0.05 mg/ml) resuspended in the respiratory buffer and incubated within the chambers of the oxygraph with 100 μM DZX and/or 500 μM 5HD during 10 min.

The ATP synthesized *in situ* was measured as described previously by Cairns *et al.* (18). Aliquots were sampled at 30-s intervals, quenched with an equal volume of 7% perchloric acid, and preserved at −80°C. The ATP content was measured from neutralized supernatants by an assay based on a tandem enzyme reaction driven by hexokinase (0.9 U/ml) and glucose-6-phosphate dehydrogenase (0.1 U/ml), which, in the presence of ATP and glucose (1 mM), converts NADP (0.5 mM) to NADPH at an equimolar ratio.

Mitochondrial enzymatic activities

The activities of the mitochondrial OXPHOS complexes (I–IV) and of the Krebs cycle enzymes in brain mitochondria were measured at 37°C on a Beckman DU-640B spectrophotometer (Beckman Coulter, Brea, CA, USA) using an adaptation of the method described by Rustin *et al.* (19). Complex V (ATP synthase) activity was measured by a coupled assay (19)

using lactate dehydrogenase and pyruvate kinase as the coupling enzymes on sonicated mitochondria (6×5 s, MSE sonicator). For the study of the mitochondrial ATP-sensitive potassium channel (mK_{ATP}) modulators, the activity was measured without FCCP to avoid IF1 binding through the loss of mitochondrial membrane potential. Complex II (succinate ubiquinone reductase) activity was measured in a reaction medium containing 50 mM phosphate buffer (pH 7.5), 2.5 mg/ml fatty acid-free BSA, 1 mM KCN, 5 μM rotenone, 5 μg/ml antimycin, 30 mM succinate, 0.1 mM 2,6-dichlorophenolindophenol (DCPIP), and 5 μg of mitochondrial proteins. After 2 min of incubation at 37°C, the reaction was initiated by addition of 0.05 mM decylubiquinone. The activity was measured at 600 nm by monitoring the reduction of DCPIP. Succinate dehydrogenase (SDH) activity was measured after the reduction of DCPIP in the presence of 1 mM phenazine methosulfate and 15 mM succinate at 600 nm (20). Specific activities were controlled using thenoyl trifluoroacetate, a succinate ubiquinone reductase inhibitor.

Protein expression

Western blotting was performed on 20 μg of brain mitochondrial proteins solubilized in a Laemmli buffer and boiled for 5 min. at 50°C. Proteins were separated on a 12.5% SDS-polyacrylamide gel and electroblotted to PVDF membranes (Amersham Biosciences, Les Ulis, France). Mouse monoclonal VDAC, complex V subunit α (55 kDa) and β (56 kDa) antibodies, and complex II subunit SDHA (70 kDa) and SDHB (30 kDa) antibodies were used for complex subunit detection (Mitosciences, Eugene, OR, USA).

Coimmunoprecipitation (CoIP) experiment

IP was performed on mitochondria from 2 mice from the same groups pooled together. As recommended by the immunocapture kit supplier (Mitosciences), 0.6 mg mitochondria diluted in PBS was solubilized by addition of 1% (w/v; 2.5 g/g mitochondrial protein) digitonin. Complex extraction and integrity were controlled by blue native-PAGE (21) on 3–12% polyacrylamide gels (Invitrogen, Carlsbad, CA, USA), and IP input was also controlled by SDS-PAGE (see above). Samples were then incubated overnight under wheel rotation at 4°C with anti-native complex I, II, or V monoclonal antibody (mAb) covalently linked to G-agarose beads (MS 101, 201, and 501c; Mitosciences) in a ratio of 60 μg Abs/mg mitochondria. Beads were then washed 3 times in either 1 mM dodecyl-maltoside (DDM) or digitonin dissolved in PBS, and elution was performed in a solution of 200 mM glycine and 1 mM DDM (pH 2.5). After neutralization, collected fractions were submitted to SDS-PAGE and electroblotted to PVDF membranes. mAbs against complex II SDHA and SDHB subunits, complex Vα and Vβ subunits, and complex I (NDUFB8), III (IIIcore2), and IV (COX1) subunits were all supplied by Mitosciences and used according to the manufacturer's recommendations. Manufacturer-supplied brain mitochondria were used as control for mAb specificity.

mK_{ATP} channel activity

Modulation of mK_{ATP} channel activity by openers (DZX) and inhibitors (5HD) was monitored spectrophotometrically (DU-640B spectrophotometer) at 520 nm, as the light-scatter (absorbance) change due to K^+ uptake, as described elsewhere (22). Respiring mitochondria take up K^+ and osmotically obligated water when suspended in K^+ medium, leading to matrix swelling. An increase in matrix volume is accompanied by a decrease in absorbance at 520 nm; which is an isosbestic point for the mitochondrial cytochromes and is therefore insensitive to changes in redox state. The mK_{ATP} K^+ buffer (100 mM KCl, 5 mM HEPES, 10 mM succinate, 10 μM rotenone, 2 μg/ml oligomycin, 100 μM EGTA, 5 mM $MgCl_2$, 2 mM KH_2PO_4, and 0.1 mg/ml BSA, pH 7.2 at 37°C) was rapidly added to a cuvette containing 0.5 mg/ml mitochondria. The change in optical density at 520 nm was recorded for 30 s, and the swelling, reflecting the increase in mK_{ATP} opening, was calculated as β, which is the inverse Δ absorbance ($1/\Delta_A$) normalized for protein concentration (23). Mitochondrial incubation in the K^+ medium induced a maximal swelling ("100%" swelling), and the new steady state of potassium influx/efflux measured after addition of inhibitors and activators is thus reported to this value (23). For control experiments (nonspecific salt transport), KCl was replaced with NaCl in the buffer. The swelling was measured immediately after the mitochondria were isolated, *i.e.*, in <1 h after brain dissection.

Statistical analysis

Statistical comparisons between control, Tg-Wt, and Tg-R94Q mice were made with the Mann-Whitney *U* test. The Wilcoxon test for paired data was used for the analysis of the effects of drugs on mitochondria. Differences were considered statistically significant at values of $P < 0.05$.

RESULTS

Mitochondrial complex II and V deficiencies in the brain mitochondria of Tg-R94Q mice

First, maximal coupled respiration, RCR, and ATP synthesis were analyzed in brain mitochondria from control, Tg-Wt, and Tg-R94Q mice (**Fig. 1*A***). ADP-stimulated (state 3) respiration driven by complex I substrates (malate and pyruvate) did not differ between Tg-R94Q, Tg-Wt, and control mice (Fig. 1*A1*). However, the addition of saturating ADP concentration failed to stimulate complex II-linked respiration in mitochondria from Tg-R94Q mice, as shown by the decrease of both the state 3 succinate-driven respiration and the RCR, *i.e.*, the ratio of oxygen consumption in the presence of ADP to that in its absence (Fig. 1*A1, 2*). In accordance with the respiratory measurements, the rate of succinate-driven ATP synthesis was reduced by nearly 80% (Fig. 1*A3*) in mitochondria from Tg-R94Q mice compared with Tg-Wt and control mice, whereas no difference was found with malate and pyruvate.

The specificity of complex II-linked respiration inhibition was further analyzed using substrates of the different complexes, alone or in combination (Fig. 1*B2*). As described above, in the presence of malate and pyruvate, ADP did stimulate respiration over state 2 (no adenylate), even in Tg-R94Q mitochondria. In control and Tg-Wt mitochondria, complex I-linked (Fig. 1*B2*, MP) and complex II-linked (Fig. 1*B2*, SR) respiration showed comparable maximal rates, while convergent electron flow from both complexes (Fig. 1*B2*, MPS) further increased coupled respiration. In Tg-R94Q mitochondria, succinate failed to stimulate respiration over malate/pyruvate but rather tended to limit the

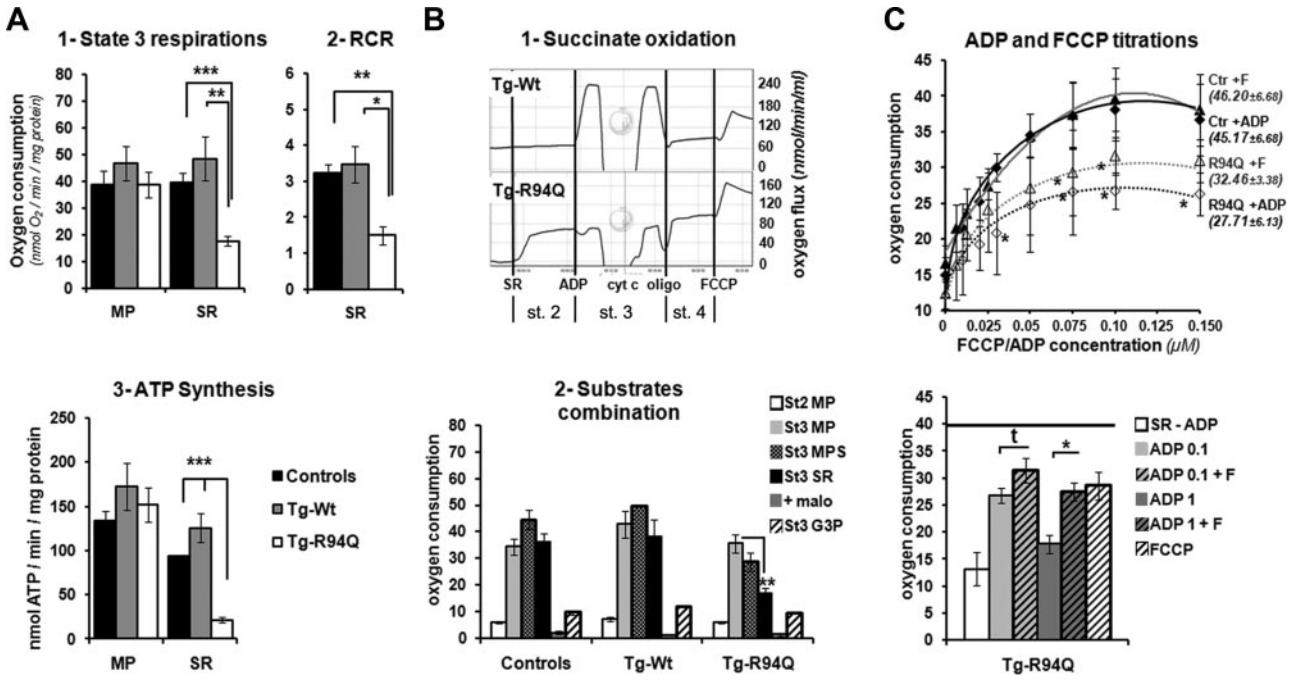

Figure 1. Major decrease in complex II-linked coupled respiration in Tg-R94Q mitochondria. *A*) Analysis of coupled respiration and phosphorylation in brain mitochondria from control, Tg-Wt, and Tg-Wt mice. *1*) State 3 oxygen consumption with complex I-dependent substrates, *i.e.*, 5 mM malate/2.5 mM pyruvate (MP; $n=5$), or complex II-dependent substrates, *i.e.*, 5 mM succinate and 10 μM rotenone (SR; $n=9$), in the presence of 0.5 mM ADP. *2*) RCR, *i.e.*, ratio of oxygen consumption in the presence of ADP to that in its absence, with complex II-dependent substrates (SR; $n=9$). *3*) Rates of mitochondrial ATP synthesis measured by spectrophotometry ($n=5$). *B*) Analysis of the specificity of the complex II-dependent state 3 inhibition. *1*) Representative oxygraphic traces of Tg-R94Q and Tg-Wt mitochondria respiring with complex II-dependent substrates, *i.e.*, 5 mM succinate and 10 μM rotenone [state 2 (st. 2)], stimulated with ADP [state 3 (st. 3)], and uncoupled with 1 μM FCCP ($n=9$). *2*) Analysis of the coupled respiration with a combination of substrates of the different complexes: malate and pyruvate (MP; complex I), malate, pyruvate, and succinate (MPS; complexes I and II), succinate and rotenone (SR; complex II, complex I inhibited), and G3P, succinate, and malonate (complex III, complex II inhibited but succinate present). St2, state 2; St3, state 3. *C*) Analysis of the respiration limitation by phosphorylation machinery. Top panel: stimulation of complex-II driven oxygen consumption rate with increasing amounts of FCCP (triangle) or ADP (square) sequentially added in the polarographic chamber. Bottom panel: respiration rates obtained with nonmaximal or maximal ADP and FCCP concentrations, alone or in combination, in mitochondria from Tg-R94Q mice. Black line represents maximal respiration of Tg-Wt and control mice. Results are expressed as means ± SE ($n=5$). $^*P < 0.05$; $^{**}P < 0.01$; $^{***}P < 0.001$.

respiration rate (Fig. 1*B2*, MPS). The respiration rate further dropped following rotenone addition (complex II-linked respiration; Fig. 1*B2*, SR). Thus, when succinate is oxidized, both states 3 (Fig. 1*B2*, MPS and SR) were lower in Tg-R94Q mitochondria than in control and Tg-Wt. Glycerol-3-phosphate (G3P) dehydrogenase and complex II both supply electrons provided by $FADH_2$ oxidation to ubiquinone and complex III. After inhibition of succinate oxidation by malonate (Fig. 1*B2*, +malo), no difference was noted between the groups using G3P as substrate. Lastly, cytochrome *c* oxydase-linked respiration did not differ either (not shown). Taken together, these data point to a specific succinate oxidation defect.

However, while ADP failed to stimulate the succinate-driven respiration in Tg-R94Q mice, uncoupling by FCCP partially reversed this inhibition (Fig. 1*B1*), suggesting that the inhibition of succinate oxidation was partially reversed when bypassing the complex V.

To further investigate this succinate oxidation defect, succinate-driven respiration was gradually stimulated by small additions of either FCCP (no adenylate added) or ADP. The FCCP titration gradually stimulates respiration by increasing proton permeability without involving the phosphorylation machinery, whereas ADP titration stimulates H^+ reentry by gradual activation of the complex V. For each value of ADP or FCCP, succinate respiration was lower in mitochondria from Tg-R94Q mice than in controls (Fig. 1*C*, top panel), pointing once again to a limitation involving complex II. However, above a threshold value, ADP failed to stimulate respiration to the level obtained with FCCP in Tg-R94Q mitochondria, while it did so in control and Tg-Wt mitochondria (Fig. 1*C*, top panel). Thus, the apparent affinity for ADP, calculated from the Lineweaver-Burk transformations, decreased 7-fold for values >0.025 mM ADP in Tg-R94Q mice (apparent K_m^{ADP} 21.8±15.6 to 154.4±41.1 μM in Tg-R94Q; Supplemental Fig. S1).

Two explanations may be proposed for this difference: an inhibitory effect of ADP on respiration or a difference due to the phosphorylation machinery [F0F1-ATP synthase, P_i carrier (PiC), or ATP/ADP translocase (ANT)]. To rule out a possible inhibition of succinate oxidation by ADP, titration of succinate-

TABLE 1. *Mitochondrial OXPHOS complex enzymatic activities*

Complex	Control	Tg-Wt	Tg-R94Q
I/CS	0.15 ± 0.023	0.18 ± 0.010	0.13 ± 0.08
II SDH/CS	0.06 ± 0.004	0.06 ± 0.006	0.04 ± 0.003***,##
II SUR/CS	0.19 ± 0.003	0.17 ± 0.07	0.15 ± 0.008**,#
III/CS	0.65 ± 0.073	0.68 ± 0.012	0.62 ± 0.032
IV/CS	2.56 ± 0.073	2.50 ± 0.0045	2.31 ± 0.090
V/CS	0.09 ± 0.005	0.14 ± 0.016*	0.06 ± 0.004**,##

Enzymatic activities of OXPHOS complexes measured in mitochondria isolated from the brain tissue of Tg-Wt, Tg-R94Q, and control mice. Values represent mean ± SE activity (nmol/min/mg protein) normalized to citrate synthase (CS). $^{*}P < 0.05$, $^{**}P < 0.01$, $^{***}P < 0.001$ *vs.* control; $^{\#}P < 0.05$, $^{\#\#}P < 0.01$ *vs.* Tg-Wt.

linked respiration with FCCP in state 3 was performed (Fig. 1*C*, bottom panel). In Tg-R94Q mitochondria, FCCP alone, or in combination with ADP, gave the same respiratory rates and always stimulated respiration to a higher rate than did ADP alone in Tg-R94Q mitochondria. This supports the hypothesis of a limitation of proton permeation at the level of the phosphorylation machinery.

Enzymatic activities of the OXPHOS complexes were then assessed in mitochondria from Tg-R94Q, Tg-Wt, and control mice (**Table 1**). No difference was found in the activities of complexes I, III, and IV. However, SDH and succinate ubiquinone reductase (SUR) activities carried out by complex II decreased by 40 and 20%, respectively ($P<0.001$) in mitochondria from Tg-R94Q mice compared with Tg-Wt and control mice. Complex V activity also decreased (30%; $P<0.01$) in Tg-R94Q compared with control mice, while it increased ($P<0.05$) in Tg-Wt compared with control mice. No difference was found in the quantity of the catalytic subunits of the 2 complexes, *i.e.*, the SDHA and SDHB subunits of complex II, and the α and β subunits of complex V (Supplemental Fig. S2 and **Fig. 2**).

SDH structurally interacts with complex V

The coexisting defect of complexes II and V observed in Tg-R94Q mice led us to analyze the possibility of a physical interaction between SDH and complex V using CoIP experiments. Mitochondria were digitonin solubilized (control inputs; Fig. 2*A*, *B*) and immunoprecipitated with anti-native F_1-ATPsynthase mAb (Fig. 2*C*), anti-native complex II mAb (Fig. 2*D*), or anti-native complex I (Fig. 2*E*). IP was followed by SDS-PAGE and immunoblotting using anti-complex II (SDHA and SDHB subunits) and anti-complex V (Vβ and Vα subunits). Both mitochondrial SDHA (the 70-kDa flavoprotein) and SDHB (the 30-kDa iron-sulfur subunit) coimmunoprecipitated with complex V (Fig. 2*C*); inversely, both subunits Vβ and Vα coimmunoprecipitated with complex II (Fig. 2*D*, Vα not shown). Neither SDH nor

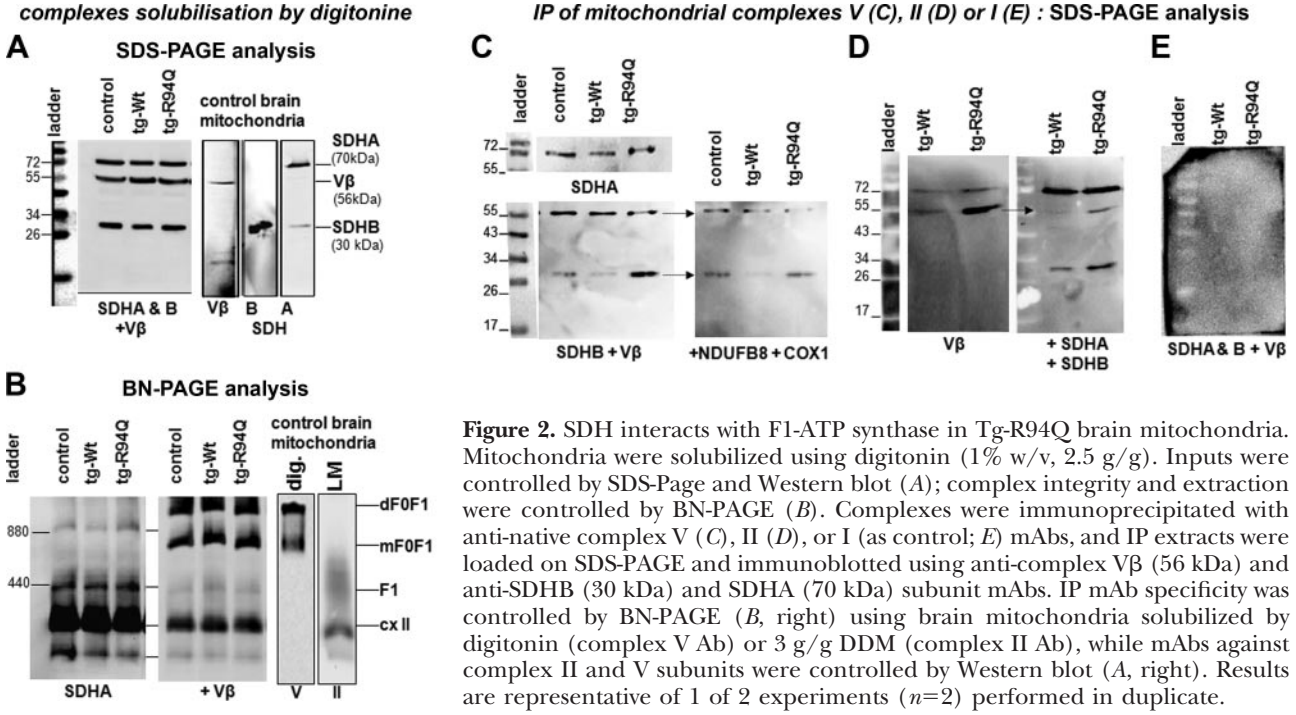

Figure 2. SDH interacts with F1-ATP synthase in Tg-R94Q brain mitochondria. Mitochondria were solubilized using digitonin (1% w/v, 2.5 g/g). Inputs were controlled by SDS-Page and Western blot (*A*); complex integrity and extraction were controlled by BN-PAGE (*B*). Complexes were immunoprecipitated with anti-native complex V (*C*), II (*D*), or I (as control; *E*) mAbs, and IP extracts were loaded on SDS-PAGE and immunoblotted using anti-complex Vβ (56 kDa) and anti-SDHB (30 kDa) and SDHA (70 kDa) subunit mAbs. IP mAb specificity was controlled by BN-PAGE (*B*, right) using brain mitochondria solubilized by digitonin (complex V Ab) or 3 g/g DDM (complex II Ab), while mAbs against complex II and V subunits were controlled by Western blot (*A*, right). Results are representative of 1 of 2 experiments ($n=2$) performed in duplicate.

Vβ/Vα bands were detected after complex I immunoprecipitation (Fig. 2*E*). Moreover, no band was detected in complex II or V CoIP experiments using anti-complex I (subunits NDUFB8, 20 kDa), anti-complex IV (COX 1, 39 kDa; Fig. 2*C*, right panel), or anti-complex III (subunit core2, not shown) antibodies. Interestingly, the intensity of SDHA and, more strikingly, SDHB bands was significantly greater in complex V IP extracts of Tg-R94Q mice compared with control and Tg-Wt mice. A higher proportion of Vβ subunits also coimmunoprecipitated with complex II in Tg-R94Q mitochondria. These results suggested either a stronger interaction between complex V and SDH proteins or a larger quantity of interacting complexes.

Complex II and V deficiencies are linked to the opening of mK_{ATP} channels

SDH has been shown to interact with complex V, ANT, PiC, and ATP-binding cassette protein 1 (ABC1) in a macromolecular supercomplex designated as the mK_{ATP} (24). Moreover, the opening of mK_{ATP} channels by DZX decreased succinate oxidation and reduced activity of complexes II and V (25–30). In Tg-R94Q mice, the functional state of mK_{ATP} channels was analyzed by the light-scatterring assay using mK_{ATP} channel modulators. A KCl buffer was used to induce maximal mitochondrial swelling as a control condition (**Fig. 3**). ATP, a known mK_{ATP} channel inhibitor, prevented this mitochondrial swelling in control, Tg-Wt, and Tg-R94Q mice (Fig. 3, top and middle panels). In Tg-Wt and control mice, the reopening of mK_{ATP} channels by DZX and the inhibition of SDH by malonate counteracted the effect of ATP, leading to mitochondrial swelling, while 5HD, an mK_{ATP} channel inhibitor, reversed the effects of DZX and malonate. In Tg-R94Q mice (Fig. 3, bottom panel), DZX and malonate failed to stimulate swelling over the level observed with ATP. Consequently, 5HD + DZX did not differ from DZX treatment in the case of Tg-R94Q mice. Surprisingly, the combination of 5HD and malonate allowed mitochondrial swelling.

As described above (Table 1), complex II (SDH) and complex V activities decreased in mitochondria from Tg-R94Q mice compared with control mice. We secondly studied the effect of mK_{ATP} channel modulators on the enzymatic activities of SDH and ATP synthase (**Fig. 4*A*, *B***). It should be noted that chemicals were first added to intact mitochondria and allowed to act for 10 min before the mitochondria were frozen. DZX decreased SDH activity of mitochondria from Tg-Wt and control mice to that of Tg-R94Q mice, as did malonate (Fig. 4*A*). The effect of DZX on the SDH activity of mitochondria from Tg-Wt and control mice was reversed by 5HD. In Tg-R94Q mitochondria, malonate and DZX could not decrease SDH activity any further, while 5HD on its own increased SDH activity to the level of mitochondria from Tg-Wt and control mice. DZX also decreased complex V activity in Tg-Wt and control

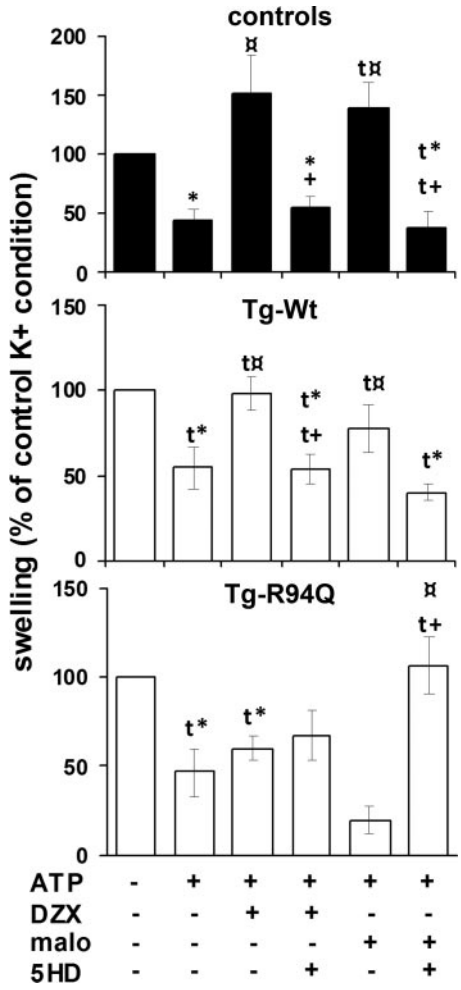

Figure 3. mK_{ATP} channel swelling/light-scatter assay in mitochondria from brain tissue of control, TgWt, and Tg-R94Q mice. Magnitude of mK_{ATP} channel swelling, normalized to control K^+ condition, as determined by a decrease in absorbance after 0.3 min incubation in K^+ medium. When indicated, 1 mM ATP, and/or 100 μM DZX, 500 μM 5HD, or 100 μM malonate were present in the medium. Results are expressed as means ± SE (controls and Tg-WT, n=5; Tg-R94Q, n=3). $^{*}P < 0.05$, $^{t*}P < 0.1$ *vs.* control; $^{\circ}P < 0.05$, $^{t\circ}P < 0.1$ *vs.* ATP; $^{+}P < 0.05$, $^{t+}P < 0.1$ *vs.* DZX or malonate.

mitochondria (Fig. 4*B*). Moreover, 5HD on its own had no effect on complex V activity in Tg-Wt and control mitochondria but restored Tg-R94Q complex V activity to the level observed in Tg-Wt and control mitochondria. In the presence of DZX, 5HD only partially increased the complex V activity in Tg-Wt and control mitochondria.

Contrary to the direct action of SDH inhibitors such as malonate, the inhibition of SDH by DZX disappeared after mitochondrial membrane disruption (freezing and thawing); the complex V inhibition by DZX was limited as well. The effect of 5HD on Tg-R94Q mitochondria also disappeared in these conditions (Supplemental Fig. S3).

Finally, the relation between succinate oxidation and mK_{ATP} channel opening was studied by polarography (Fig. 4*C*). As reported above, state 3 succinate respira-

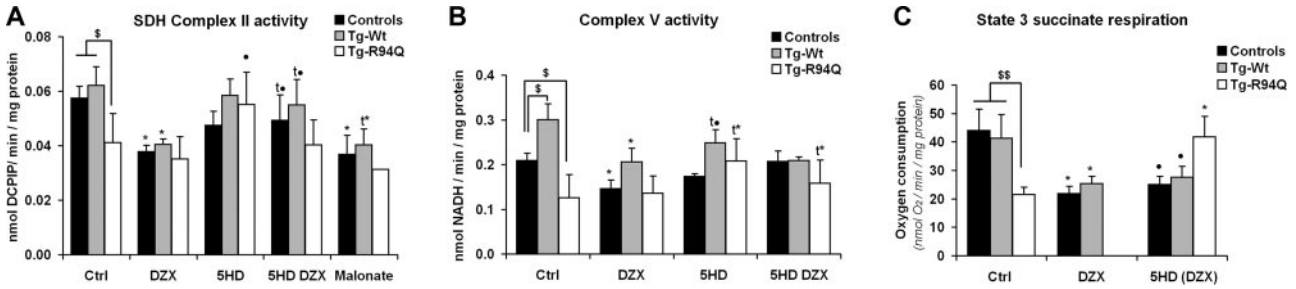

Figure 4. Effect of mK_{ATP} modulators on SDH complex II activity (*A*), complex V activity (*B*), and state 3 succinate-driven respiration rate (*C*). *A, B*) SDH complex II (*A*) and complex V (*B*) mitochondrial enzymatic activities measured in brain mitochondria from control, Tg-Wt, and Tg-R94Q mice after incubation with 100 μM DZX, 500 μM 5HD, or 100 μM malonate as indicated. Activities were normalized to citrate synthase (CS; $n=5$). *C*) State 3 oxygen consumption with complex II-dependent substrates, measured in mitochondria isolated from brain tissue of control, Tg-Wt, and Tg-R94Q mice in control conditions (DMSO treatment); in the presence of 100 μM DZX ($n=5$); and, in the last condition, in the presence of DZX + 500 μM 5HD (controls and Tg-Wt; $n=5$) or 5HD only (Tg-R94Q, $n=3$). Results are expressed as means ± SE (nmol/min/mg protein). $^{*}P < 0.05$, $^{t*}P < 0.1$ *vs.* control; $^{\bullet}P < 0.05$, $^{t\bullet}P < 0.1$ *vs.* DZX; $^{\$}P < 0.05$, $^{\$\$}P < 0.01$ *vs.* Tg-Wt.

tion was greatly decreased in Tg-R94Q mitochondria compared with Tg-Wt and control mitochondria. In Tg-Wt and control mitochondria, DZX decreased specifically the state 3 succinate-related respiration to the level observed in Tg-R94Q mitochondria. Consequently, the RCR with succinate as substrate did not differ any longer between mitochondria from Tg-Wt or control mice after the addition of DZX (1.18±0.10 and 1.47±0.34, respectively) and Tg-R94Q mice (1.51±0.76). 5HD fully restored ADP-stimulated succinate oxidation in Tg-R94Q mitochondria. However, as for complex V activity, the decrease in succinate oxidation caused by DZX in Tg-Wt and control mitochondria was only partially restored. The respiratory rates were higher with DZX + 5HD than with DZX alone in Tg-Wt and control mitochondria but did not attain normal respiratory values.

DISCUSSION

MFN2 plays a central role in mitochondrial outer-membrane fusion and in the regulation of mitochondrial energetic metabolism. Metabolic explorations of cell models carrying *MFN2* mutations responsible for CMT2A disease argue in favor of an energetic defect participating in the pathogenesis of the disorder (10, 12, 13). We investigated mitochondrial energetic metabolism in a recently developed transgenic mouse model carrying the p.R94Q mutation, one of the most frequent human MFN2 mutations, which reproduces the peripheral neuropathy (15).

Our results show for the first time that an *MFN2* mutation leads to a bioenergetic impairment in brain. None of the defects were observed in the transgenic mouse expressing the human nonmutated *MFN2* cDNA, which excludes any effect linked to the slight MFN2 overexpression (15). In Tg-R94Q mice, both SDH and SUR were decreased (40 and 20%, respectively). This complex II deficiency was combined with a complex V deficiency (30% decrease), which in turn greatly reduced succinate-related ATP synthesis. Impaired complex II and V activities were not linked to modifications of complex V assembly or content.

Interestingly, the succinate oxidation decrease in brain mitochondria from Tg-R94Q mice was revealed by the activation of complex V, since it was essentially observed during maximal coupled respiration (phosphorylation). Indeed, above an ADP threshold concentration of ~0.025 mM, the affinity of succinate-supported respiration for ADP was strongly reduced. This defect could be partially reversed when bypassing complex V. Indeed, the uncoupler FCCP, alone or in combination with ADP, stimulated succinate-driven respiration over state 3 in mitochondria from Tg-R94Q mice, while ADP, FCCP, or both gave the same respiration rates in mitochondria from Tg-Wt or control mice. This points to the phosphorylation machinery as a limiting step and is consistent with an involvement of complex V. More strikingly, impaired phosphorylation of ADP is only observed when complex II substrate, *i.e.*, succinate, is oxidized. This inhibition could not rely on a direct inhibition of respiration by succinate, since the presence of this substrate did not reduce respiration when the SDH inhibitor malonate is also added (Fig. 1*B2*, see state 3 G3P condition). Altogether, the functional analyses pointed to a succinate oxidation defect in brain Tg-R94Q mitochondria, revealed by the complex V activation or, inversely, an inactivation of the phosphorylation machinery by succinate oxidation. Due to the decrease in both complex V activity and ATP synthesis, which suggests a limitation of phosphorylation by ATP synthase, we focused our study on this complex. However, ANT and PiC also play an important role in phosphorylation regulation by supplying substrates (ADP and P_i) for ATP synthesis. ANT and PiC have been shown to form, with ATP synthase, the ATP synthasome responsible for the terminal step of ATP synthesis in mitochondria (25). Thus, we cannot rule out the possibility that these two carriers also participate in the limitation of phosphorylation in Tg-R94Q mitochondria.

Although combined SDH and complex V deficiencies have been reported in humans (26), there have been very few reports to date in the literature concerning a possible interaction between SDH and ATP synthase/ATP synthasome. Interestingly, SDH has been shown to associate with complex V, ANT, PiC, and ABC1 to form a macromolecular complex displaying a K^+ transport activity that is sensitive to known mK_{ATP} modulators (24), and ANT has been shown to mediate the mK_{ATP}-opener-induced potassium flux to the mitochondrial matrix (27). Moreover, short repetitive ischemic episodes or the administration of DZX decreased succinate oxidation without affecting NADH oxidation in mitochondria isolated from rat and pig heart tissues (28–31). Decreased SDH activity has also been described, in these conditions, in the heart and cultured cortical neurons of rats (30, 32). To sum up, ischemic and pharmacological preconditioning conditions linked to mK_{ATP} channel activation mimic the impairment of the mitochondrial metabolism observed in Tg-R94Q mitochondria, *i.e.*, the succinate oxidation defect and complex II and V inhibition. Conversely, all known SDH inhibitors, *i.e.*, malonate, 3-nitropropionic acid, and atpenin A5, are shown to mediate protection from ischemia by the activation of mK_{ATP} channels (32–34). Complex V has also been described as a target for DZX (35, 36), which favors complex V inhibition through the protein inhibitor of F1 (IF1; ref. 37). The hypothesis emerging from these studies is that the activities of complexes II and V, on the one hand, and mK_{ATP} channel opening, on the other, are inversely related. A main reason would be that the same proteins are involved in both processes that would be mutually exclusive.

The results of the CoIP experiments performed on wild-type brain mitochondria extracts strongly suggest the existence of a physical association between complexes II and V, an association that would be reinforced in Tg-R94Q mitochondria. In mitochondria from these mice, the defects of complexes II and V were associated with an altered functional state of mK_{ATP} channels. DZX, a specific mK_{ATP} channel opener, and malonate, an SDH inhibitor, induced a K^+-dependent mitochondrial swelling in mitochondria from Tg-Wt and control mice but had no effect on mitochondria from Tg-R94Q mice. This could be linked to the lower enzymatic SDH activity that we found in mitochondria from Tg-R94Q mice. These results suggest that the mK_{ATP} could not be further stimulated in these mitochondria, probably because the target by which DZX activates the mKATP opening is already occupied or activated. DZX, when added to Tg-Wt and control mitochondria, decreased the enzymatic activities of complexes II and V to the level of those in Tg-R94Q mitochondria (**Fig. 5**). However, it did not affect these enzymatic activities in Tg-R94Q mitochondria. With DZX, the phosphorylating succinate-driven respiration was therefore inhibited at the same level as Tg-R94Q respiration.

Moreover, 5HD, the mK_{ATP} inhibitor, fully reversed the effect of DZX on complex II activities in Tg-Wt and

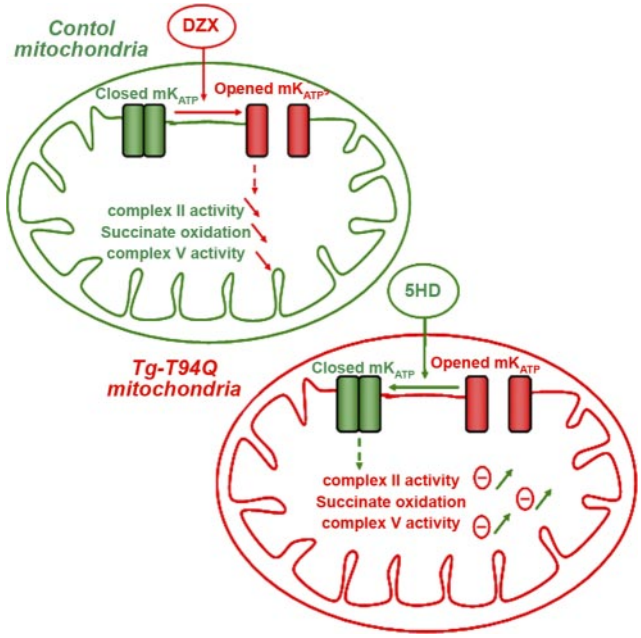

Figure 5. Diagram representing the hypothesized effects of mK_{ATP} channel modulators on mitochondrial SDH activity, complex V activity, and state 3 succinate-driven respiration. In Tg-R94Q mice, both complex II and V activities were impaired, which greatly reduced the coupled respiration linked to complex II substrate. In these mitochondria, the mK_{ATP} channel inhibitor 5HD allows restoration of complex II and V activities and succinate oxidation. Inversely, in mitochondria from control mice, the mK_{ATP} activator DZX induces a decrease in complex II and V activity and in succinate oxidation, mimicking the Tg-R94Q phenotype.

control mitochondria. This clearly links the action of DZX on SDH to the opening of mK_{ATP} channels (Fig. 5). However, 5HD only partially counteracted the effects of DZX on complex V activity and succinate oxidation in the presence of ADP. This suggested that one part of the DZX action on complex V activity is not specific to mK_{ATP} channels. Interestingly, in Tg-R94Q mitochondria, 5HD fully restored succinate oxidation and the activities of complexes II and V.

To sum up, DZX, an mK_{ATP} channel stimulator, mimicked the impaired biochemical phenotype observed in Tg-R94Q mitochondria, while 5HD, an mK_{ATP} channel inhibitor, restored the impaired biochemical phenotype (Fig. 5). These results argue in favor of higher rate/state of mK_{ATP} channel opening in Tg-R94Q mitochondria. It is important to note that the effects of DZX and 5HD on SDH activity in Tg-R94Q and control mitochondria require the structural integrity of mitochondrial membranes, arguing for specific effects on an mK_{ATP} macromolecular complex.

The results demonstrate a dominant negative effect of the R94Q Mfn2 mutation, leading to an mKATP opening and an OXPHOS defect, which is likely to participate to the pathophysiology of CMT2A. The mechanism linking mutated MFN2 to mK_{ATP} opening and OXPHOS defect remains to be elucidated.

A direct interaction of MFN2 (outer mitochondrial membrane) with the respiratory chain and the mK_{ATP}

(inner mitochondrial membrane) is unlikely, since the large majority of MFN2 is exposed to the cytosol, and only a weak portion of the protein is located in the intermembrane space. However, although the energetic defect involves reactions taking place exclusively on the inner membrane, MFN2 has previously been shown to interact with a protein located in this membrane (38). Moreover, some studies have reported that the intermembrane space loop of Fzo1, the MFN2 yeast ortholog, is an important domain for its interaction with the mitochondrial inner membrane (39, 40).

The MFN2 mutation may also activate one of the mK_{ATP} regulatory pathways, one of which is the calcium/IP3 pathway. Recently, a role of MFN2 protein in tethering endoplasmic reticulum mitochondria has been described (41), and the silencing of *MFN2* has been shown to disrupt efficient mitochondrial Ca^{2+} uptake (41). In addition, mK_{ATP} activity is especially affected by changes in the volume of the mitochondrial matrix. An increase in mitochondrial density was observed in the distal axons of Tg-R94Q mice (15) and was attributed to an increase in the number of fission events leading to an increased number of organelles without affecting the total mitochondrial mass. Such variations of mitochondrial size could induce a contraction of the mitochondrial matrix, in turn activating the mK_{ATP} channels.

In summary, this study constitutes the first demonstration of oxidative phosphorylation impairment in the neuronal cells of a CMT2A mouse model. The results also strongly argue in favor of functional links between complexes II and V within the mK_{ATP} channel, links that are rarely evoked despite the abundant literature concerning the supercomplexes of the respiratory chain. Interestingly, mK_{ATP} channels are particularly abundant in the brain, with 6 or 7 times more mK_{ATP} channels than in other tissues (42). This could partly explain the neurospecificity of CMT2A. These results reveal a new neuropathogenic mechanism underlying the energetic impairment related to the activation of mK_{ATP} channels that could open new therapeutic perspectives. FJ

This work was supported by the Institut National de la Santé et de la Recherche Médicale (INSERM), the University Hospital of Angers (PHRC 04-12), the University of Angers, and grants from the following associations of patients: Association Contre les Maladies Mitochondriales (AMMi), Retina France, Ouvrir les Yeux (OLY), and Union Nationale des Aveugles et Déficients Visuel (UNADEV). The authors are grateful to C. Wetterwald, to the technicians of the laboratory for technical assistance, and to Kanaya Malkani for critical reading and comments on the manuscript.

REFERENCES

1. Skre, H. (1974) Genetical and clinical aspects of Charcot-Marie-Tooth's disease. *Clin. Genet.* **6,** 98–118
2. Züchner, S., Mersiyanova, I. V., Muglia, M., Bissar-Tadmouri, N., Rochelle, J., Dadali, E. L., Zappia, M., Nelis, E., Patitucci, A., Senderek, J., Parman, Y., Evgrafov, O., Jonghe, P. D., Takahashi, Y., Tsuji, S., Pericak-Vance, M. A., Quattrone, A., Battaloglu, E., Polyakov, A. V., Timmerman, V., Schröder, J. M., and Vance, J. M. (2004) Mutations in the mitochondrial GTPase mitofusin 2 cause Charcot-Marie-Tooth neuropathy type 2A. *Nat. Genet.* **36,** 449–451
3. Chan, D. C. (2006) Mitochondrial fusion and fission in mammals. *Annu. Rev. Cell Dev. Biol.* **22,** 79–99
4. Okamoto, K., and Shaw, J. M. (2005) Mitochondrial morphology and dynamics in yeast and multicellular eukaryotes. *Annu. Rev. Genet.* **39,** 503–536
5. Chen, H., Detmer, S. A., Ewald, A. J., Griffin, E. E., Fraser, S. E., and Chan, D. C. (2003) Mitofusins Mfn1 and Mfn2 coordinately regulate mitochondrial fusion and are essential for embryonic development. *J. Cell Biol.* **160,** 189–200
6. Verhoeven, K., Claeys, K. G., Züchner, S., Schröder, J. M., Weis, J., Ceuterick, C., Jordanova, A., Nelis, E., De Vriendt, E., Van Hul, M., Seeman, P., Mazanec, R., Saifi, G. M., Szigeti, K., Mancias, P., Butler, I. J., Kochanski, A., Ryniewicz, B., De Bleecker, J., Van den Bergh, P., Verellen, C., Van Coster, R., Goemans, N., Auer-Grumbach, M., Robberecht, W., Milic Rasic, V., Nevo, Y., Tournev, I., Guergueltcheva, V., Roelens, F., Vieregge, P., Vinci, P., Moreno, M. T., Christen, H. J., Shy, M. E., Lupski, J. R., Vance, J. M., De Jonghe, P., and Timmerman, V. (2006) MFN2 mutation distribution and genotype/phenotype correlation in Charcot-Marie-Tooth type 2. *Brain* **129,** 2093–2102
7. Vallat, J. M., Ouvrier, R. A., Pollard, J. D., Magdelaine, C., Zhu, D., Nicholson, G. A., Grew, S., Ryan, M. M., and Funalot, B. (2008) Histopathological findings in hereditary motor and sensory neuropathy of axonal type with onset in early childhood associated with mitofusin 2 mutations. *J. Neuropathol. Exp. Neurol.* **67,** 1097–1102
8. Detmer, S. A., and Chan, D. C. (2007) Complementation between mouse Mfn1 and Mfn2 protects mitochondrial fusion defects caused by CMT2A disease mutations. *J. Cell Biol.* **176,** 405–414
9. Baloh, R. H., Schmidt, R. E., Pestronk, A., and Milbrandt, J. (2007) Altered axonal mitochondrial transport in the pathogenesis of Charcot-Marie-Tooth disease from mitofusin 2 mutations. *J. Neurosci.* **27,** 422–430
10. Loiseau, D., Chevrollier, A., Verny, C., Guillet, V., Gueguen, N., Pou de Crescenzo, M. A., Ferré M, Malinge, M. C., Guichet, A., Nicolas, G., Amati-Bonneau, P., Malthièry, Y., Bonneau, D., and Reynier, P. (2007) Mitochondrial coupling defect in Charcot-Marie-Tooth type 2A disease. *Ann. Neurol.* **61,** 315–323
11. Amiott, E. A., Lott, P., Soto, J., Kang, P. B., McCaffery, J. M., DiMauro, S., Abel, E. D., Flanigan, K. M., Lawson, V. H., and Shaw, J. M. (2008) Mitochondrial fusion and function in Charcot-Marie-Tooth type 2A patient fibroblasts with mitofusin 2 mutations. *Exp. Neurol.* **211,** 115–127
12. Bach, D., Pich, S., Soriano, F. X., Vega, N., Baumgartner, B., Oriola, J., Daugaard, J. R., Lloberas, J., Camps, M., Zierath, J. R., Rabasa-Lhoret, R., Wallberg-Henriksson, H., Laville, M., Palacín, M., Vidal, H., Rivera, F., Brand, M., and Zorzano, A. (2003) Mitofusin-2 determines mitochondrial network architecture and mitochondrial metabolism. A novel regulatory mechanism altered in obesity. *J. Biol. Chem.* **278,** 17190–17197
13. Pich, S., Bach, D., Briones, P., Liesa, M., Camps, M., Testar, X., Palacín, M., and Zorzano, A. (2005) The Charcot-Marie-Tooth type 2A gene product, Mfn2, up-regulates fuel oxidation through expression of OXPHOS system. *Hum. Mol. Genet.* **14,** 1405–1415
14. Cartoni, R., and Martinou, J. C. (2009) Role of mitofusin 2 mutations in the physiopathology of Charcot-Marie-Tooth disease type 2A. *Exp. Neurol.* **218,** 268–273
15. Cartoni R, Arnaud E, Médard JJ, Poirot O, Courvoisier DS, Chrast R, and Martinou, J. C. (2010). Expression of mitofusin 2(R94Q) in a transgenic mouse leads to Charcot-Marie-Tooth neuropathy type 2A. *Brain* **133**, 1460–1469
16. Kijima, K., Numakura, C., Izumino, H., Umetsu, K., Nezu, A., Shiiki, T., Ogawa, M., Ishizaki, Y., Kitamura, T., Shozawa, Y., and Hayasaka, K. (2005) Mitochondrial GTPase mitofusin 2 mutation in Charcot-Marie-Tooth neuropathy type 2A. *Hum. Genet.* **116,** 23–27
17. Neusch, C., Senderek, J., Eggermann, T., Elolff, E., Bähr, M., and Schneider-Gold, C. (2007) Mitofusin 2 gene mutation (R94Q) causing severe early-onset axonal polyneuropathy (CMT2A). *Eur. J. Neurol.* **14,** 575–577

18. Cairns, C. B., Walther, J., Harken, A. H., and Banerjee, A. (1998) Mitochondrial oxidative phosphorylation thermodynamic efficiencies reflect physiological organ roles. *Am. J. Physiol.* **274,** R1376–1383
19. Rustin, P., Chretien, D., Bourgeron, T., Gérard, B., Rötig, A., Saudubray, J. M., and Munnich, A. (1994) Biochemical and molecular investigations in respiratory chain deficiencies. *Clin. Chim. Acta* **228,** 35–51
20. Hederstedt, L., Heden, L. O. (1989) New properties of Bacillus subtilis succinate dehydrogenase altered at the active site. *Biochem. J.* **260,** 491–497
21. Wittig, I., Braun, H. P., and Schägger, H. (2006) Blue native PAGE. *Nat. Protoc.* **1,** 418–428
22. Wojtovich, A. P., and Brookes, P. S. (2008) The endogenous mitochondrial complex II inhibitor malonate regulates mitochondrial ATP-sensitive potassium channels, implications for ischemic preconditioning. *Biochim. Biophys. Acta* **1777,** 882–889
23. Costa, A. D., Quinlan, C. L., Andrukhiv, A., West, I. C., Jabůrek, M., and Garlid, K. D. (2006) The direct physiological effects of mitoK(ATP) opening on heart mitochondria. *Am. J. Physiol. Heart Circ. Physiol.* **290,** 406–415
24. H, Chen, Z., Ko, Y., Mejía-Alvarez, R., and Marbán, E. (2004) Multiprotein complex containing succinate dehydrogenase confers mitochondrial ATP-sensitive K^+ channel activity. *Proc. Natl. Acad. Sci. U. S. A.* **101,** 11880–11885
25. Ko, Y. H., Delannoy, M., Hullihen, J., Chiu, W., and Pedersen, P. L. (2003) Mitochondrial ATP synthasome. Cristae-enriched membranes and a multiwell detergent screening assay yield dispersed single complexes containing the ATP synthase and carriers for Pi and ADP/ATP. *J. Biol. Chem.* **278,** 12305–12309
26. Brière, J. J., Favier, J., El Ghouzzi, V., Djouadi, F., Bénit, P., Gimenez, A. P., and Rustin, P. (2005) Succinate dehydrogenase deficiency in human. *Cell Mol. Life Sci.* **62,** 2317–2324
27. Kopustinskiene, D. M., Toleikis, A., and Saris, N. E. (2003) Adenine nucleotide translocase mediates the K(ATP)-channel-openers-induced proton and potassium flux to the mitochondrial matrix. *J. Bioenerg. Biomembr.* **35,** 141–148
28. Hanley, P. J., Mickel, M., Löffler, M., Brandt, U., and Daut, J. (2002) K(ATP) channel-independent targets of diazoxide and 5-hydroxydecanoate in the heart. *J. Physiol.* **542,** 735–741
29. Lim, K. H., Javadov, S. A., Das, M., Clarke, S. J., Suleiman, M. S., and Halestrap AP. (2002) The effects of ischaemic preconditioning, diazoxide and 5-hydroxydecanoate on rat heart mitochondrial volume and respiration. *J. Physiol.* **545,** 961–974
30. Pasdois, P., Beauvoit, B., Tariosse, L., Vinassa, B., Bonoron-Adèle, S., and Santos, P. D. (2006) MitoK(ATP)-dependent changes in mitochondrial volume and in complex II activity during ischemic and pharmacological preconditioning of Langendorff-perfused rat heart. *J. Bioenerg. Biomembr.* **38,** 101–112
31. Schäfer, G., Wegener, C., Portenhauser, R., and Bojanovski, D. (1969) Diazoxide, an inhibitor of succinate oxidation. *Biochem. Pharmacol.* **18,** 2678–2681
32. Kis, B., Rajapakse, N. C., Snipes, J. A., Nagy, K., Horiguchi, T., and Busija, D. W. (2003) Diazoxide induces delayed pre-conditioning in cultured rat cortical neurons. *J. Neurochem.* **87,** 969–980
33. Horiguchi, T., Kis, B., Rajapakse, N., Shimizu, K., and Busija, D. W. (2003) Opening of mitochondrial ATP-sensitive potassium channels is a trigger of 3-nitropropionic acid-induced tolerance to transient focal cerebral ischemia in rats. *Stroke* **34,** 1015–1020
34. Wojtovich, A. P., and Brookes, P. S. (2009) The complex II inhibitor atpenin A5 protects against cardiac ischemia-reperfusion injury via activation of mitochondrial KATP channels. *Basic Res. Cardiol.* **104,** 121–129
35. Ala-Rämi, A., Ylitalo, K. V., and Hassinen, I. E. (2003) Ischaemic preconditioning and a mitochondrial KATP channel opener both produce cardioprotection accompanied by F1F0-ATPase inhibition in early ischaemia. *Basic Res. Cardiol.* **98,** 250–258
36. Comelli, M., Metelli, G., and Mavelli, I. (2007) Downmodulation of mitochondrial F0F1 ATP synthase by diazoxide in cardiac myoblasts, a dual effect of the drug. *Am. J. Physiol. Heart Circ. Physiol.* **292,** H820–829
37. Contessi, S., Metelli, G., Mavelli, I., and Lippe, G. (2004) Diazoxide affects the IF1 inhibitor protein binding to F1 sector of beef heart F0F1ATPsynthase. *Biochem. Pharmacol.* **67,** 1843–1851
38. Guillery, O., Malka, F., Landes, T., Guillou, E., Blackstone, C., Lombès, A., Belenguer, P., Arnoult, D., and Rojo, M. (2008) Metalloprotease-mediated OPA1 processing is modulated by the mitochondrial membrane potential. *Biol. Cell* **100,** 315–325
39. Fritz, S., Rapaport, D., Klanner, E., Neupert, W., and Westermann, B. (2001) Connection of the mitochondrial outer and inner membranes by Fzo1 is critical for organellar fusion. *J. Cell Biol.* **152,** 683–692
40. Neuspiel, M., Zunino, R., Gangaraju, S., Rippstein, P., and McBride, H. (2005) Activated mitofusin 2 signals mitochondrial fusion, interferes with Bax activation, and reduces susceptibility to radical induced depolarization. *J. Biol. Chem.* **280,** 25060–25070
41. De Brito, O. M., and Scorrano, L. (2008) Mitofusin 2 tethers endoplasmic reticulum to mitochondria. *Nature* **456,** 605–610
42. Bajgar, R., Seetharaman, S., Kowaltowski, A. J., Garlid, K. D., and Paucek, P. (2001) Identification and properties of a novel intracellular (mitochondrial) ATP-sensitive potassium channel in brain. *J. Biol. Chem.* **276,** 33369–33374

Received for publication September 23, 2010.
Accepted for publication January 21, 2011.